

Proposal of an extended t - J Hamiltonian for high- T_c cuprates from *ab initio* calculations on embedded clusters

Carmen J. Calzado* and Jean-Paul Malrieu

Laboratoire de Physique Quantique, IRSAMC, Université Paul Sabatier, 31062 Toulouse, France

(Received 17 October 2000; revised manuscript received 17 November 2000; published 15 May 2001)

A series of accurate *ab initio* calculations on Cu_pO_q finite clusters, properly embedded in the Madelung potential of the infinite lattice, have been performed in order to determine the local effective interactions in the CuO_2 planes of $\text{La}_{2-x}\text{Sr}_x\text{CuO}_4$ compounds. The values of the first-neighbor interactions, magnetic coupling ($J_{NN}=125$ meV), and hopping integral ($t_{NN}=-555$ meV) have been confirmed. Important additional effects are evidenced, concerning essentially the second-neighbor hopping integral $t_{NNN}=+110$ meV, the displacement of a singlet toward an adjacent colinear hole, $h_{SD}^{abc}=-80$ meV, a non-negligible hole-hole repulsion $V_{NN}-V_{NNN}=0.8$ eV, and a strong anisotropic effect of the presence of an adjacent hole on the values of the first-neighbor interactions. The dependence of J_{NN} and t_{NN} on the position of neighbor hole(s) has been rationalized from the two-band model and checked from a series of additional *ab initio* calculations. An extended t - J model Hamiltonian has been proposed on the basis of these results. It is argued that the here-proposed three-body effects may play a role in the charge/spin separation observed in these compounds, that is, in the formation and dynamic of stripes.

DOI: 10.1103/PhysRevB.63.214520

PACS number(s): 74.72.-h, 74.25.Ha, 74.25.Jb

I. INTRODUCTION

The insulating cuprates, such as La_2CuO_4 , which are the undoped parent compounds of the high- T_c superconductor $\text{La}_{2-x}\text{Sr}_x\text{CuO}_4$, are known to present antiferromagnetic couplings between nearest-neighbor (NN) copper centered sites in the CuO_2 planes. Raman and neutron-diffraction experiments evaluate this coupling to be around $J_{NN}=130$ meV [128 ± 6 meV,^{1,2} 134 ± 5 meV,³⁻⁵ respectively]. Nevertheless, the corresponding simple Heisenberg Hamiltonian does not reproduce entirely the features of the Raman spectrum⁶⁻¹¹ and additional effects such as second-neighbor magnetic coupling J_{NNN} and four-spin cyclic exchange have been invoked.¹²⁻¹⁵ While an upper bond for J_{NNN} ($|J_{NNN}|\leq 9$ meV) has been given from Raman experiments,⁵ the amplitude of the four-spin operator in this kind of compounds is a matter of discussion. Previous works have shown that this cyclic operator corresponds to a fourth-order term in the perturbative expansion of the Hubbard model Hamiltonian, scaling as $\lambda t_{NN}^4/U^3$, where t_{NN} is the nearest-neighbor hopping integral and U is the on-site Coulombic repulsion, with $\lambda=40$ (Refs. 16 and 17) or $\lambda=80$,^{18,19} depending on the formal writing of the Hamiltonian.

Regarding the hole-doped material, where the conduction takes place in the CuO_2 planes, the holes can be seen as centered on copper atoms with large tails on the four neighboring oxygen atoms. They move from one site to an adjacent one through the effect of a hopping operator of amplitude t_{NN} , for which there is no direct experimental evaluation, but values around -0.5 eV are considered as reasonable.²⁰ One of the most widely employed model Hamiltonians for the interpretation of the properties of these materials, through a hole-pairing mechanism, is the so-called t - J model^{21,22} which combines spin coupling and hole hopping:

$$H = \sum_{ab} J_{NN} \cdot (S_a \cdot S_b - 1/4) + t_{NN} \cdot (a_a^\dagger a_b + a_b^\dagger a_a + \text{s.c.}) \delta(n_a + n_b, 1). \quad (1)$$

The adequacy of such a simple Hamiltonian to incorporate the physics of the problem is questionable. Hopping between second-neighbor sites, t' , may be non-negligible. When one derives the t - J Hamiltonian from the Hubbard Hamiltonian, three-site operators moving a singlet-coupled electron pair toward the hole appear at second order of perturbation theory, scaling as the J_{NN} operator, i.e., as t_{NN}^2/U . The transferability of J_{NN} from the undoped to the doped material is not guaranteed, the presence of a neighboring hole may affect the coupling of two adjacent spins. The hole-hole repulsion V_{ij} is likely to play a role, influencing the mean distance between the holes. Different extensions of the t - J model have been employed in numerical simulations, for instance, t - t' - J (Refs. 23-26) or t - J - V ,²⁷⁻²⁹ but the values given to the parameters are rather arbitrary, varying widely from one author to the other, the main objective being to exhibit qualitative collective effects. Among them the experimental evidence of the occurrence of stripes have focused attention in the recent past.³⁰

The goal of the present paper is to bring useful information regarding the local effective interactions in undoped and hole-doped cuprates. To obtain them, the most accurate tools of *ab initio* quantum chemistry will be used. The method consists in considering few-site clusters, properly embedded in the field of the periodic environment, and to calculate the low part of the spectrum using the exact Hamiltonian, large basis sets, and extensive configuration interaction (CI) expansions. From this spectrum it is possible to fix the amplitudes of the effective interactions. The procedure has been successfully used to calculate the NN magnetic coupling in a series of perovskites,³¹ among them La_2CuO_4 for which a

value of $J_{NN}=130$ meV is obtained. Similar calculations of the hopping integral in the hole-doped system ($t=-0.57$ eV) have been also reported.^{32,33} These calculations concerned symmetrical two-site clusters, for which the determination of J_{NN} and t_{NN} is straightforward from the two lowest eigenvalues. This is no longer the case when one considers larger clusters to extract additional parameters, concerning next-nearest-neighbor (NNN) interactions, neighboring-hole dependence of J_{NN} and t_{NN} , hole-hole repulsions, and four-spin cyclic operators. Their achievement requires some additional mathematical tools such as the Bloch definition³⁴ of effective Hamiltonians and localization procedures (for instance, the Boys method³⁵). The methodology will be explained in Sec. II. Section III will present the results concerning the four-site square plaquette and three-site linear cluster with different number of electrons (holes). Calculations performed on undoped clusters provide the values of the NN, NNN, and next NNN magnetic couplings. Also the amplitude of the four-spin cyclic exchange for this compound has been established. Hole-doped clusters give informations about the hopping integrals (NN, NNN, and next NNN), the singlet-displacement operator and the dependence of the first-neighbor interactions (hopping integral and magnetic exchange) on the number and relative position of the adjacent holes. Section V presents a rationalization of the anisotropy of the effect of hole(s) in the vicinity on the values of J_{NN} and t_{NN} and reports additional exploratory calculations to evaluate the dependence of the bicentric parameters on the hole positions. Finally, Sec. VI summarizes the results, proposing a refined t - J model, and discusses the possible effect of the additional operators on the charge/spin distribution on the lattice, with possible consequences for the stripping phenomena.

II. METHOD

A. Mapping of a model Hamiltonian on an *ab initio* effective Hamiltonian

For such materials the unpaired electrons are essentially located on Cu dx^2-y^2 in-plane atomic orbitals, with non-negligible delocalization tails on the adjacent oxygen atoms. Such Cu-centered orbitals will be labeled $\{a, b, c, \dots\}$. In the doped material the hole has much larger delocalization tails on O $2p$ orbitals, but as shown by Zhang and Rice,^{21,22} it remains possible to work within a one-band model Hamiltonian, the precise nature of its valence orbitals being implicit. For a finite cluster involving p centers and $n \leq p$ unpaired electrons, the model Hamiltonian acts in the subspace spanned by the localized determinants ϕ_i , containing a common frozen *core* and n active electrons. The double occupancy of the active orbitals of these localized determinants is prohibited in both the Heisenberg and the t - J Hamiltonians.

The *ab initio* calculations handle a large number of atomic orbitals, symmetry-adapted molecular orbitals (MO's), and expansions of the wave functions on millions of determinants. Nevertheless, it is possible to construct from these calculations *ab initio* effective Hamiltonians which are in one-to-one correspondence with the model Hamiltonians.

For an undoped cluster involving p Cu atoms (p sites), it is possible first to obtain from variational calculations a set of molecular orbitals containing doubly occupied MO's (*core*), unoccupied MO's (*virtual* MO's), and p MO's with essentially single occupation, which define the *ab initio* one-electron valence space, $\{\varphi_i\}$ in Fig. 1. A unitary localizing transformation of the p symmetry-adapted orbitals will provide equivalent localized orbitals $\{a', b', c', \dots\}$ which can be seen as in strict one-to-one correspondence with the implicit valence orbitals of the model Hamiltonian. This localizing unitary transformation \mathcal{U} may be evident by symmetry or defined by a localizing functional, for instance, the Boys criterion (see Sec. III A), $\{a', b', c', \dots\} = \mathcal{U}\{\varphi_p, \varphi_q, \dots\}$. Fixing a double occupancy of the *core* orbitals, and putting n electrons in the valence localized orbitals, avoiding their double occupation, localized neutral determinants $\{\phi'_{i,loc}\}$, are obtained which are in correspondence with the n -electron basis of the model Hamiltonian. These localized neutral determinants can be written as

$$\phi'_{i,loc} = |\text{core } (a' b' c' \dots)| * S_i, \quad (2)$$

where S_i is one of the $C_p^{p/2}$ spin distributions on the various active localized orbitals. These determinants define a model space (of projector P_S , $P_S = \sum |\phi'_{i,loc}\rangle \langle \phi'_{i,loc}|$) for the *ab initio* calculations. Let N_S be the dimension of that space S . The information obtained by the most refined *ab initio* calculations will be extracted according to the theory of the effective Hamiltonian proposed by Bloch.³⁴ When one knows the N_S eigenstates Ψ_m having the *largest projections* on the model space (which constitute the target space, stable subspace of H_{exact}) and their eigenvalues E_m , the effective Hamiltonian is such that its eigenvalues are the exact ones, and its eigenvectors are the projections of the exact eigenvectors onto the model space:

$$H^{eff} |P_S \Psi_m\rangle = E_m |P_S \Psi_m\rangle, \quad m = 1, N_S. \quad (3)$$

The spectral definition of H^{eff} is

$$H^{eff} = \sum_m |P_S \Psi_m\rangle E_m \langle P_S \Psi_m^\perp|, \quad (4)$$

where $|P_S \Psi_m^\perp\rangle$ is the biorthogonal transformation of $|P_S \Psi_m\rangle$. Actually the projections $|P_S \Psi_m\rangle$ of the (orthogonal) states Ψ_m have no reason (except for symmetry reasons) to be orthogonal; they define an overlap matrix s ,

$$s_{mn} = \langle P_S \Psi_m | P_S \Psi_n \rangle, \quad (5)$$

and the biorthogonal vectors are defined by

$$|P_S \Psi_m^\perp\rangle = s^{-1} |P_S \Psi_m\rangle. \quad (6)$$

The values of the norms of the projections, i.e., the diagonal elements of s matrix, give an indication on the quality of the description of these states by the truncated space S . The model space and the exact eigenstates must be in strong correspondence, i.e., one must choose both spaces so that the vectors Ψ_m have the largest projections on the model space.

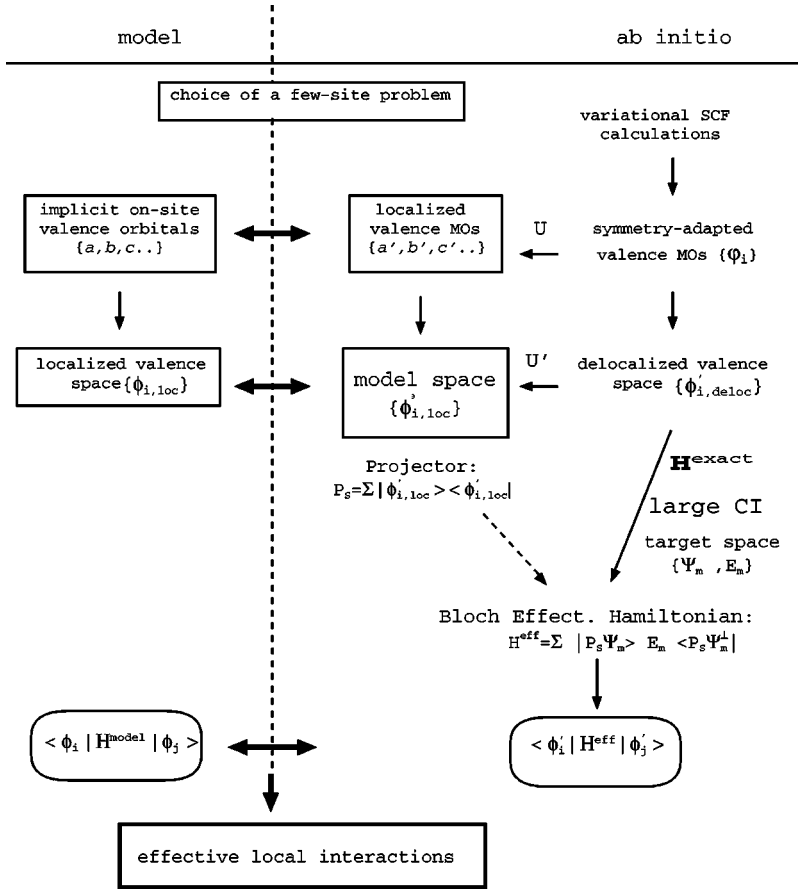


FIG. 1. Summary of the strategy used to extract effective interactions in $\text{La}_{2-x}\text{Sr}_x\text{CuO}_4$ systems.

Then one may express this Hamiltonian on the basis of the localized determinants $\{\phi'_{i,loc}\}$ written in terms of the orbitals $\{a', b', c', \dots\}$ and the matrix elements

$$\langle \phi'_{i,loc} | H^{eff} | \phi'_{j,loc} \rangle = \sum_m \langle \phi'_{i,loc} | P_S \Psi_m \rangle E_m \langle P_S \Psi_m^\dagger | \phi'_{j,loc} \rangle \quad (7)$$

can be identified to the matrix elements $\langle \phi_i | H | \phi_j \rangle$ of the model Hamiltonian. Since the symmetry-adapted delocalized determinants $\{\phi'_{i,deloc}\}$ are linear combinations of the localized neutral determinants $\{\phi'_{i,loc}\}$, constituting two basis sets of the same model space,

$$|\phi'_{i,deloc}\rangle = \sum_k d_{i,k} |\phi'_{k,loc}\rangle, \quad (8)$$

it is not difficult to calculate the overlap:

$$\langle \phi'_{i,loc} | P_S \Psi_m \rangle = \sum_j \langle \phi'_{i,loc} | \phi'_{j,deloc} \rangle c_{m,j}, \quad (9)$$

where $c_{m,j}$ is the coefficient of the $|\phi'_{j,deloc}\rangle$ determinant on the $|P_S \Psi_m\rangle$ wave function.

In principle the effective Hamiltonians may be non-Hermitian but the hermitization is straightforward.³⁶ The comparison between the *ab initio* effective Hamiltonian and the model Hamiltonian fixes the amplitudes of the integrals appearing in the latter and allows one to verify whether non-

negligible additional interactions are not present. Figure 1 summarizes the whole process. Changing the size of the cluster, for instance going from a two-center/one-electron problem to a three-center/two-electron one, one may check the consistency of the procedure and the transferability of the effective interactions.

B. Computational details

The widely used embedded cluster technique has been employed to model the system.^{37–42} Finite clusters of the type Cu_pO_q (Cu_3O_{10} and Cu_4O_{12} , Fig. 2) have been selected, where the q oxygen atoms are the first in-plane neighbors of the p Cu atoms. (Previous calculations have shown that the explicit involvement of the out-of-plane oxygen atoms does not change the values of the in-plane interactions.^{32,33}) The first shell of atoms surrounding the cluster have been replaced by formal charges with pseudopotentials, in order to mimic the Coulombic and exclusion effects. The rest of the lattice has been modeled by means of point charges, which values have been fixed according to Evjen's method,⁴³ and which correctly represent the Madelung potential of the crystal.⁴⁴ This is a simplified approach in comparison with more elaborate methods proposed in the literature.⁴⁵

The ten most internal electrons of Cu atoms have been represented by effective core pseudopotentials, the valence electrons being treated explicitly with triple- ζ basis sets.⁴⁶ A double- ζ basis set has been used for oxygen

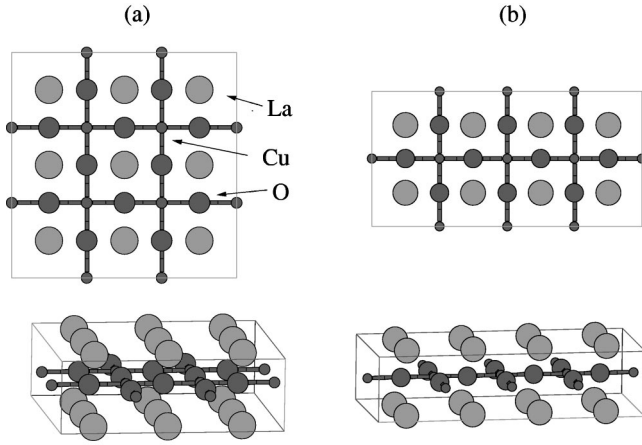


FIG. 2. Representation of the clusters employed in the *ab initio* calculations. (a) the plaquette Cu_4O_{12} ; (b) the linear cluster Cu_3O_{10} . The first-neighbors of the cluster atoms have been also included. They have been modeled by means of the combination of a pseudopotential and a point charge, to mimic both the exclusion and the Coulombic effects.

atoms,⁴⁶ preliminary calculations on bicentric clusters have shown that the inclusion of polarization functions on the bridging oxygen atoms has not an important effect either on the magnetic coupling or on the hopping integral.

For undoped clusters, the restricted-spin open-shell Hartree-Fock calculations variationally define the singly occupied magnetic orbitals. These orbitals define a minimal valence complete active space (CAS). From this space it is possible to calculate the spectrum through a difference dedicated configuration interaction (DDCI) procedure⁴⁷ which implies all the simple and double excitations on the top of this CAS, except the double excitations from the *core* to the *virtual* orbitals, which do not contribute to the energy difference at second-order of perturbation theory.⁴⁷

An alternative solution consists in defining an enlarged CAS including the on-bond $2p$ orbital of the bridging oxygen atoms. These ligand-centered orbitals are the most participating on the intersite spin-exchange and electron transfer processes.⁴⁸ Performing all the single excitations on the top of this extended CAS, which corresponds to the two-band Hubbard model space, one introduces dynamical polarization effects, i.e., screening by the nonactive electrons, at lower computational cost than the preceding computational scheme. For such type of systems, the equivalence of the DDCI procedure on the top of the small CAS and the single excitations on the top of the enlarged CAS, including the most relevant ligand orbitals, has been illustrated on the La_2CuO_4 system (using a Cu_2O_7 cluster)^{33,49} and on oxalato-bridged Cu(II) complexes.^{49,50}

III. AB INITIO CALCULATIONS ON THE PLAQUETTE AND THE LINEAR CLUSTERS

As was mentioned above, two different clusters have been used to extract the effective interactions. A four-site square cluster (plaquette) of formula Cu_4O_{12} [Fig. 2(a)] has been employed in order to determine the first- (NN) and second-

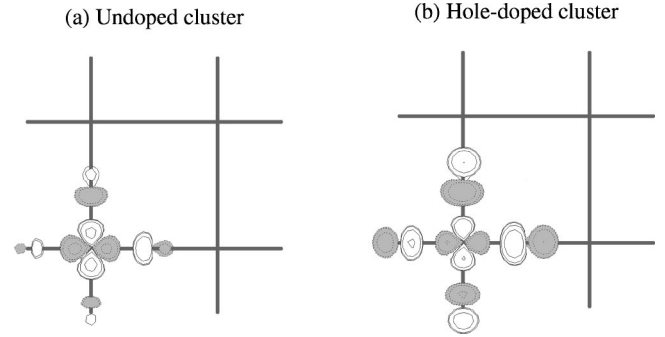


FIG. 3. Localized active orbitals for the plaquette: (a) for undoped systems, centered in $3d_{x^2-y^2}$, with important tails on the four in-plane neighbor oxygen atoms; (b) for hole-doped systems a strong $3d-2p$ rehybridization takes place, the $2p$ character increases substantially with respect to the undoped situation.

neighbor (NNN) interactions, and also the four-spin cyclic exchange. Third-neighbor interactions (nNNN) has been estimated by means of the calculations carried out in a linear three-site cluster [Cu_3O_{10} , Fig. 2(b)]. Comparing with the results obtained from the plaquette and previously studied binuclear clusters, it is possible to check the dependence of the NN interactions on the size of the fragment involved in the *ab initio* calculations.

Three fillings of the *valence shell* have been considered in order to evaluate the dependence of these interactions on the hole concentration. Undoped (four center/four electron and three center/three electron problems), one hole-doped ($4c/3e$ and $3c/2e$), and two hole-doped ($4c/2e$ and $3c/1e$) situations have been analyzed. From the systems with two holes in the valence shell, it is possible to extract the amplitude of the hole-hole repulsions, an important magnitude for the study of the hole pairing mechanism. It is worthwhile to notice that the here-referred hole dopings are not in correspondence with the total doping of the lattice, induced by the replacement of La^{+3} by Sr^{+2} . A change in the occupation of the valence shell of these small clusters just induces a *local* hole doping, which provides information about the *local* modifications of the effective parameters.

A. Localization process

In the plaquette, the four symmetry-adapted valence orbitals belong to the A_{1g} , E_u , and B_{1g} representations in the D_{4h} group. The localizing unitary transformation is straightforward since

$$a_{1g} = (a + b + c + d)/2, \quad (10)$$

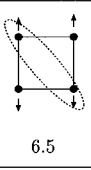
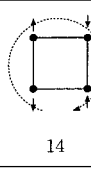
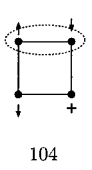
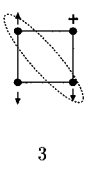
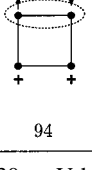
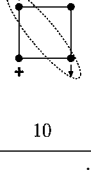
$$e_{u(1)} = (a + b - c - d)/2, \quad (11)$$

$$e_{u(2)} = (a - b - c + d)/2, \quad (12)$$

$$b_{1g} = (a - b + c - d)/2. \quad (13)$$

Figure 3 pictures one of these four localized valence orbitals for undoped and for the doped plaquettes, showing the strong localization of the magnetic orbitals and the $d-p$ hybridization occurring in the hole-doped systems.^{32,33,44,51}

TABLE I. Magnetic interactions in undoped and hole-doped clusters (in meV).

	J_{NN}	J_{NNN}	J_{nNNN}	K
Undoped clusters	 125 ^a			
	 122		 1	
	 124	 6.5		 14
	Exp.	128±6 ^b , 134±5 ^c	≤ 9 ^d	-
Doped clusters	 156		 -11	
	 104	 3		
	 94	 10		

^aA value of $J_{NN}=130$ meV has been previously reported (Refs. 32 and 33), where polarization functions have been included in the basis set of the bridge oxygen atom.

^bRefs. 1 and 2.

^cRefs. 3–5.

^dRef. 5.

In the linear cluster the localizing transformation of the three magnetic orbitals is no longer imposed by the symmetry. Two of these orbitals (φ_g, φ'_g) belong to the A_g irreducible representation and the other one (φ_u) to the B_{1u} symmetry. The rotation U , which transforms the $\{\varphi_g, \varphi'_g, \varphi_u\}$ into the localized set $\{a', b', c'\}$, has been performed according to the Boys criterion,³⁵ which maximizes the distance between the centroids of the orbitals. An alternative localization criterion, the minimization of the direct exchange integral K_{ac} , leads to the same rotation.

B. Magnetic interactions

Table I reports the results obtained from the plaquette and the linear clusters for the magnetic coupling, involving different fillings of the valence shell. For the undoped cluster, the first-neighbor magnetic coupling J_{NN} is ~ 125 meV. The calculated value is independent on the size of the considered

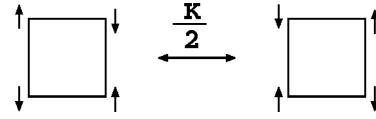


FIG. 4. Cyclic permutation of the four spins on the plaquette, showing the action of the K operator.

cluster and it is in agreement with both the previously determined J_{NN} in the binuclear cluster, by using *ab initio* configuration interaction techniques^{31–33,40} or the density-functional theory,⁴² and the estimations from Raman and neutron-diffraction experiments [128 ± 6 meV,^{1,2} 134 ± 5 meV,^{3–5} respectively]. This independence of J_{NN} with respect to the size of the cluster is in accord with the previous work of Illas *et al.*,⁴¹ performed at a level which only recovers 70% of the experimental value of J_{NN} (see also Ref. 39), due to the neglect of the polarization effects of the ligand to metal charge-transfer (LMCT) forms in the CI calculations.

The coupling between second neighbors J_{NNN} is also antiferromagnetic, with a value of $J_{NNN}=6.5$ meV in accordance with the experimental upper limit $|J_{NNN}| \leq 9$ meV.⁵ The ratio of the NNN and NN interactions is $J_{NNN}/J_{NN}=0.052$, in good agreement with the value accepted by Lorenzana *et al.*¹³ in numerical simulations, $J_{NNN}/J_{NN}=0.04$. A negligible antiferromagnetic coupling has been found between Cu atoms placed at a $2R$ distance (third neighbors, next NNN): $J_{nNNN}=1$ meV.

Finally, the calculations on the plaquette provide a non-negligible value for the four-spin cyclic exchange of $K=14$ meV. The four-body operator can be written as

$$H_K = K \sum_{\langle ijkl \rangle} [(S_i \cdot S_j)(S_k \cdot S_l) + (S_i \cdot S_l)(S_j \cdot S_k) - (S_i \cdot S_k) \times (S_j \cdot S_l)]. \quad (14)$$

This operator produces the cyclic permutation of the four spins on the plaquette (Fig. 4) plus ordinary two-spin exchanges of all the pairs of spins of the plaquette including those of the diagonals. Its value is somewhat smaller than some estimations used in numerical simulations,^{14,13,52} but larger than the critical value, $(K/J_{NN})_c = 0.05 \pm 0.04$, estimated by Sakai and Hasegawa¹⁵ for the appearance of a magnetization plateau at half the saturation value in the $S = \frac{1}{2}$ antiferromagnetic spin ladders. In spite of the smallness of the here-proposed value of the four-spin cyclic exchange, it could affect the fitting of the experimental data, as it happens in the two-leg spin ladders in the $\text{La}_6\text{Ca}_8\text{Cu}_{24}\text{O}_{41}$ system, where the best fit to the experimental data of the $w-Q$ dispersion is obtained when a value of the cyclic exchange about 10% of the main Cu-O-Cu linear exchange is included into the Hamiltonian.⁵³

When a hole is introduced in the cluster, the NN magnetic coupling is influenced by its presence, but in different directions depending on the relative position of this hole (Table I). Thus a hole in a colinear position to the two NN spins *increases* the coupling between these two spins [Fig. 5(a)]. However the NN magnetic coupling *diminishes* if the hole is placed in a position perpendicular to the bond [Fig. 5(b)].

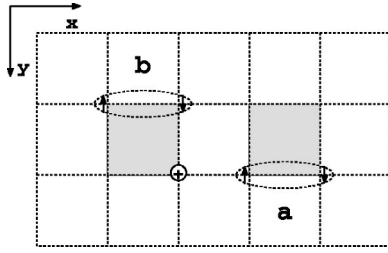


FIG. 5. Relative position of two coupled electrons with respect to an adjacent hole: (a) colinear position; (b) perpendicular position.

The same trend is observed in the plaquette when a second hole is introduced, J_{NN} being 94 meV, to be compared with $J_{NN}=104$ meV in presence of one hole and $J_{NN}=125$ meV for undoped systems.

C. Hopping integrals

As in the case of magnetic interactions, the first-neighbor hopping integral (t_{NN}) is also independent on the size of the cluster (Table II), a value of -558 meV has been found in the one-hole-doped linear cluster, -552 meV in the one-hole-doped plaquette and -555 meV in a previously reported binuclear cluster.^{32,33} This value is in accordance with a generally accepted value of -500 meV for these compounds²⁰ (for instance, -570 meV by Wang *et al.*,⁵⁴ -650 by Martin,⁴⁴ -400 meV by Hybertsen *et al.*⁵⁵).

An evaluation of second- and third-neighbor hopping integrals results from our calculations. The NNN hopping integral $t_{NNN}=+112$ meV is unexpectedly large. The sign is in agreement with the negative overlap of the active orbitals placed at a $\sqrt{2}R$ distance, but its magnitude is large due to through-bond processes, which involve the oxygen atoms. On the basis of the perturbation theory (quasidegenerated perturbation theory, QDPT),^{34,36,56} considering the neutral valence bond as the model space and H_0 being the trace of the Hamiltonian in the basis of the single determinants, there are two contributions to the t_{NNN} hopping integral. One corresponds to a third-order contribution,⁵⁷ scaling as $-t_{pp}(t_{pd})^2/\Delta E_{CT}^2$, where t_{pd} is the hopping integral between the O $2p$ and the Cu $3d$ orbitals, t_{pp} is the hopping integral between the O $2p$ orbitals, and ΔE_{CT} is the O $2p \rightarrow$ Cu $3d$ charge-transfer excitation energy (Fig. 6). Since t_{pp} , t_{pd} , and ΔE_{CT} are negative quantities, the third-order contribution results in a positive magnitude. There exists an alternative pathway corresponding to a fourth-order contri-

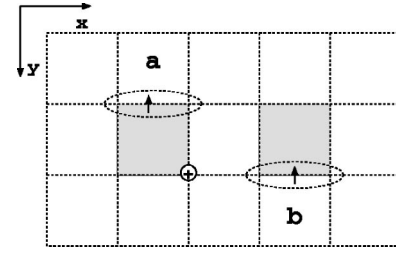


FIG. 7. Relative position of an electron delocalized between two adjacent sites, with respect to an additional hole: (a) perpendicular situation; (b) colinear situation.

bution, scaling as $t_{pd}^4/\Delta E_{CT}^3$, with opposite sign. Since the third-order contribution is expected to be larger than the fourth-order one, the resulting sign of t_{NNN} is positive.

A moderate amplitude of the hopping integral between third neighbors (t_{nNNN} , distance $2R$) has been extracted from the calculations on the linear cluster. The extension of this coupling is controlled by through-bond interactions, but in contrast with the plaquette, the third order contribution will be negligible ($t_{pp} \sim 0$) and only fourth-order processes can be written here, smaller in magnitude and with an opposite sign with respect to t_{NNN} .

When an additional hole is introduced in the system, the NN hopping integral is unchanged when the hole is placed in a perpendicular position to the bond [$t_{NN} = -558$ meV in the two-hole-doped plaquette, Fig. 7(a)], but its absolute value is augmented when the hole is placed in a colinear position to the bond [$t_{NN} = -600$ meV in the two-hole-doped linear cluster, Fig. 7(b)]. The presence of the extra hole does not influence significantly either the second-neighbor ($t_{NNN} = +130$ meV to be compared with $+112$ meV in absence of this additional hole) or the third-neighbor ($t_{nNNN} = -36$ meV versus -47 meV) hopping integrals.

D. Singlet displacement operator

Additional information coming from these calculations concerns the singlet-displacement operator (Table III). It is a three-site/two-electron operator, which moves the pair of electrons, coupled in a singlet, toward a hole placed in a neighbor position. Thus a singlet on sites a and b , the site c containing a hole, is displaced to the positions b and c , the hole being in a (Fig. 8).

It can be written as

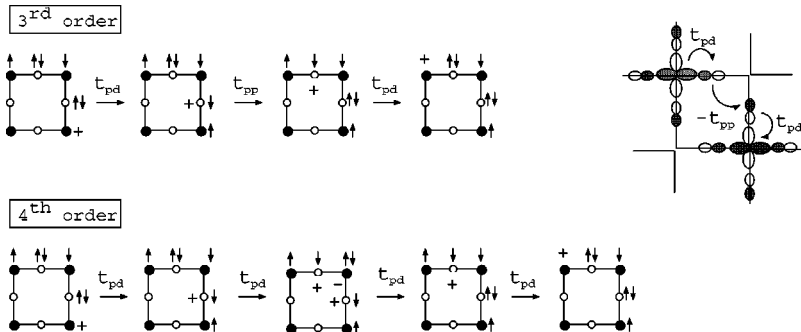
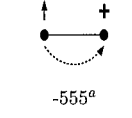
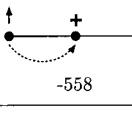
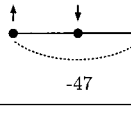
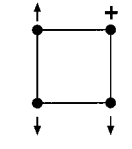
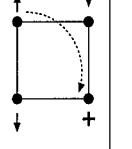
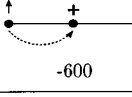
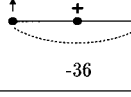
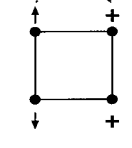
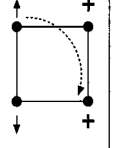


FIG. 6. Pathways showing the third-order and fourth-order perturbative contributions to the second-neighbor hopping integral, t_{NNN} . On the corner, a schematic representation illustrating the hopping processes between oxygen and the metal atoms (t_{pd}) and between two adjacent oxygen atoms (t_{pp}), and precisising the sign convention.

TABLE II. Hopping integrals. Dependence on the presence and the position of an additional hole (in meV).

	t_{NN}	t_{NNN}	t_{nNNN}
1 Hole-doped clusters	 -555 ^a		
	 -558		 -47
	 -552	 +112	
2 Hole-doped clusters	 -600		 -36
	 -558	 +130	

^aRefs. 32 and 33.

$$h_{SD}^{abc} [|a\bar{b} - \bar{a}b\rangle \langle b\bar{c} - \bar{b}c| + |b\bar{c} - \bar{b}c\rangle \langle a\bar{b} - \bar{a}b|] \delta(n_a + n_b + n_c, 2), \quad (15)$$

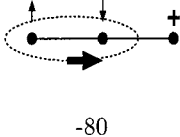
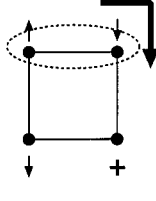
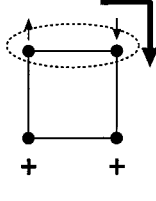
where $\delta(n_a + n_b + n_c, 2)$ controls the fact that the three centers bear only two electrons, i.e., that the singlet can only move toward a hole. As for the preceding parameters, the amplitude h_{SD}^{abc} depends on the relative position of the hole. When the singlet moves to a neighbor bond in the plaquette (i.e., the hole is placed in a perpendicular position to the singlet bond), the value is $h_{SD}^{abc} = -41$ meV while it goes to $h_{SD}^{abc} = -80$ meV when the hole is on the same axis as the singlet. The presence of a second hole in the plaquette does not affect the amplitude of the singlet displacement ($h_{SD}^{abc} = -37$ meV).

There exists also a small similar operator involving the diagonal of the square ($h_{SD}^{abd} = 9$ meV),

$$h_{SD}^{abd} [|b\bar{c} - \bar{b}c\rangle \langle b\bar{d} - \bar{b}d| + |b\bar{d} - \bar{b}d\rangle \langle b\bar{c} - \bar{b}c|] \delta(n_b + n_c + n_d, 2), \quad (16)$$

moving the electrons as shown in Fig. 9. The value of this operator in presence of a second hole is very close to the preceding value: $h_{SD}^{abd} = 14$ meV.

TABLE III. Singlet-displacement operator (in meV). Effect of the presence of a second hole in the neighborhood of the singlet.

	h_{SD}^{\perp}	h_{SD}^{\parallel}
1 Hole-doped clusters		 -80
	 -41	
2 Hole-doped clusters	 -37	

E. Hole-hole repulsions

The absolute value of the hole-hole repulsion is not accessible, but the effective Hamiltonian gives the difference between two situations (Table IV). From the plaquette, we can extract the relative stability of two holes placed in NNN positions with respect to two holes in NN:

$$V_{NN} - V_{NNN} = V_{ab} - V_{ac} = 0.98 \text{ eV}. \quad (17)$$

This is significantly larger than the values usually accepted for simulations.²⁷⁻²⁹ One should stress the fact that this value takes into account the dynamical repolarization effects of all the atoms explicitly treated in the calculation, i.e., the screening by the 12 in-plane oxygen atoms linked to the four Cu atoms of the plaquette. It misses the polarization of the rest of the environment. This effect can be evaluated taking into account the polarization of a large surrounding shell, with a value of the polarizability of the $\text{O}^=$ ion, $\alpha_{\text{O}} = 1.30 \text{ \AA}^3$. This value has been obtained from a series of finite-field *ab initio* calculations on an embedded CuO_4 cluster and it is in agreement with experimental estimates.⁵⁸ The environment polarization energy corresponding to the situation represented by $\phi'_{i,loc}$ can be written as

$$E_{pol}(\phi'_{i,loc}) = \sum_{\text{O}_p \in \text{cluster}} -\frac{1}{2} \alpha_{\text{O}} F_p^2(i'), \quad (18)$$

where $\vec{F}_p(i')$ is the electric field created by the holes in $\phi'_{i,loc}$ on the position of atom p . Including the polarization effects for the two situations (two holes in NN and in NNN positions) results in a decrease of the hole-hole repulsion difference to $V_{NN} - V_{NNN} = 0.80$ eV which remains a rather large value. From the linear cluster, it is possible to estimate the energy gain obtained when placing two holes in nNNN positions (distance $2R$) instead of adjacent positions (distance R): $V_{NN} - V_{nNNN} = V_{ab} - V_{ac} = 1.77$ eV, with a final value of $V_{NN} - V_{nNNN} = 1.47$ eV once the environment polarization effects have been taken into account.

These values of *differences* between hole-hole repulsions may seem very large and most of the calculations introducing this repulsion in a t - J - V model usually take smaller values ($J < V < 4J$)²⁷⁻²⁹ when looking for the hole-pairing mechanism. The above calculated values are smaller than the corresponding electrostatic quantities calculated in a point-charge approximation: $V_{NN} - V_{NNN} = 1.12$ eV and $V_{NN} - V_{nNNN} = 1.90$ eV. The delocalization of the holes on the oxygen atoms should result in larger repulsions, especially for V_{NN} since the two holes share an oxygen atom, and our values, which exhibit a significant screening, do not seem unrealistic.

IV. INTERPRETATION OF THE HOLE DEPENDENCE OF THE ONE BOND J_{NN} AND t_{NN} PARAMETERS

The two preceding sections indicate that the presence of holes in the immediate vicinity of a bond may affect the values of the spin coupling and of the hopping integral on this bond, and that this effect is anisotropic, i.e., does not only depend on the minimal distance of the hole to the atoms of the bond. Hence it seems important to rationalize these effects if possible.

A. Rationalization from the two-band model

1. Hopping integral

The rationalization of this anisotropy is possible in terms of the two-band model. The t hopping integral results from a second-order effect (Fig. 10), t scaling as

$$t \sim \frac{t_{pd}^2}{\Delta E_{CT}}, \quad (19)$$

where ΔE_{CT} is the $2p$ O to $3d$ Cu charge-transfer excitation energy, that is, the energy difference between the charge transfer and the model space states. In presence of an additional hole, the energies of the model space determinants ϕ_1 and ϕ_2 and of the intermediate charge-transfer state ϕ_{CT} will be modified. The model space determinant energies are no longer degenerate and one shall take their mean energy as the zero-order energy. Let consider now the effect on the bond directed along x of an adjacent hole placed either on the y direction, as occurs in the plaquette, or on the x axis, as in the linear cluster [Figs. 7(a) and 7(b), respectively]. In the situation of Fig. 7(a), the change of the zero-order mean electrostatic energy due to the hole is $\delta E_0 = (\sqrt{2} + 1)/2\sqrt{2}R = 0.85/R$. In the corresponding charge-transfer state the

mean electrostatic energy with the hole is $\delta E_{CT} = 2/\sqrt{5}R = 0.89/R$, i.e., the excitation energy $\Delta E'_{CT}$ is increased by a small quantity,

$$\Delta E'_{CT} = \Delta E_{CT} + \delta E_{CT} - \delta E_0 = \Delta E_{CT} + \frac{0.04}{R}, \quad (20)$$

which should diminish slightly the absolute value of the hopping integral. In contrast, for the situation of Fig. 7(b), $\delta E_0 = 3/4R$ and $\delta E_{CT} = 2/3R$ hence $\Delta E'_{CT} = \Delta E_{CT} - 0.08/R$ which should increase the absolute value of t , in agreement with our calculation.

This analysis is quite rudimentary, it neglects the possible effects of the polarization of the orbitals on the t_{pd} integrals and rests on a crude evaluation of the electrostatic effects on the denominators (holes considered as centered on Cu sites, neglecting their oxygen character), but it seems to agree with the computed trends.

2. Magnetic coupling

The same kind of analysis may be attempted for the J_{NN} coupling constant. In the two-band model, the spin exchange between Cu_a and Cu_b results from an interaction through the bridge oxygen atoms. In a first step an electron is transferred between the oxygen atom and one of the Cu atoms. In Fig. 11 the open circle represents a bridge oxygen atom and closed circles are the copper atoms as in Fig. 10. The top pathway corresponds to an electron transfer between the oxygen and the Cu_a atom. On the bottom pathway, the oxygen electron jumps in the opposite direction, toward the Cu_b atom. In absence of a hole in the neighborhood, both situations have the same energy: $\Delta E_{CT1} = \Delta E_{CT2} = \Delta E_{CT}$.

In the next step, an electron is transferred from the Cu atom (b in the top pathway, a in the bottom) to the oxygen atom. Notice that the resulting determinants are the ionic forms $|a\bar{a}\rangle$ and $|b\bar{b}\rangle$, which energies U_1 and U_2 corresponding to the Coulombic repulsion of two electrons placed in the same $3d$ orbital are equal in the undoped system, $U_1 = U_2 = U$. Following this perturbative development, the magnetic coupling is a fourth-order quantity:

$$\frac{J_{NN}}{2} = \frac{-2t_{pd}^4}{U(\Delta E_{CT})^2}. \quad (21)$$

Adding an external hole will not modify the electrostatic zero-order energy, but will affect the energies of all intermediate states, so that the coupling becomes

$$\frac{J_{NN}}{2} = \frac{-t_{pd}^4}{\Delta E_{CT1}^2} \cdot \frac{1}{U_1} + \frac{-t_{pd}^4}{\Delta E_{CT2}^2} \cdot \frac{1}{U_2}, \quad (22)$$

where the first term corresponds to the top pathway and the second term to the bottom one. Notice that while $\Delta E_{CT1} = \Delta E_{CT} + \delta E_{CT1}$ and $\Delta E_{CT2} = \Delta E_{CT} + \delta E_{CT2}$ have no reason to be related, $U_1 = U + \delta U$ and $U_2 = U - \delta U$ whatever the outer charge distribution. The effective coupling is therefore

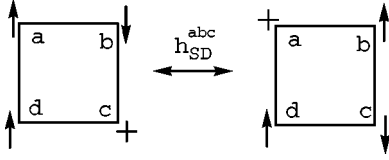


FIG. 8. Schematic representation of the singlet-displacement operator. The local singlet $a\bar{b}$ is displaced to $b\bar{c}$, the hole moving from c site to a site.

$$\frac{J_{NN}}{2} = -t_{pd}^4 \left(\frac{1}{(\Delta E_{CT} + \delta E_{CT1})^2} \cdot \frac{1}{U + \delta U} + \frac{1}{(\Delta E_{CT} + \delta E_{CT2})^2} \cdot \frac{1}{U - \delta U} \right). \quad (23)$$

To the first order in $\delta U/U$ and $\delta E_{CT}/\Delta E_{CT}$ developments, one gets

$$\frac{J_{NN}}{2} = \frac{-2t_{pd}^4}{U(\Delta E_{CT})^2} \left(1 - \frac{\delta E_{CT1}}{\Delta E_{CT}} - \frac{\delta E_{CT2}}{\Delta E_{CT}} - \frac{\delta U}{U} + \frac{\delta U}{U} \right) + \mathcal{O}(2). \quad (24)$$

The effect of the additional hole(s) will go through their electrostatic interaction in the charge-transfer states. For the perpendicular situation (Fig. 12) $\delta E_{CT1} = 0.187/R$ and $\delta E_{CT2} = -0.105/R$. Hence, $\delta E_{CT1} + \delta E_{CT2} = 0.082/R$ and J_{NN} is diminished by the presence of the adjacent hole in the perpendicular direction, as observed in the corresponding *ab initio* calculations ($\Delta J_{NN}/J_{NN} = -17\%$).

Oppositely, in the linear situation the quantities are: $\delta E_{CT1} = 1/6R$ and $\delta E_{CT2} = -1/3R$, so $\delta E_{CT1} + \delta E_{CT2} = -1/6R$ is a negative quantity, hence the coupling constant should be increased. This is actually observed since $\Delta J_{NN}/J_{NN} = +25\%$. The variation of J_{NN} in the linear model is of the right sign and its amplitude is larger than for the perpendicular orientation.

3. Singlet-displacement operator

The same kind of rationalization applies to the two-electron/three-center operator h_{SD}^{abc} . In the one-band model as shown in Fig. 13, where only the Cu atoms have been included, the electron placed in site a is transferred to site b , followed by a second transfer toward c .

TABLE IV. Hole-hole repulsions (in eV). Values in parentheses take into account the polarizability of the outer environment

$V_{NN} - V_{N\bar{N}N}$	$V_{NN} - V_{n\bar{N}N\bar{N}}$
 0.98(0.8)	 1.77(1.47)

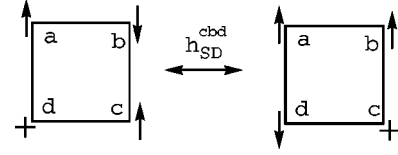


FIG. 9. The singlet-displacement operator acting over the diagonal of the plaquette.

This effect scales as t_{NN}^2/U' , where $U' = U - 2V_{ab} + V_{ac}$, V_{ij} being the electrostatic interaction between the charges (with respect to the basic undoped distribution). The denominator will be smaller for the linear configuration than for the perpendicular one since V_{ac} is larger ($1/\sqrt{2}R$ instead of $1/2R$). This may explain the difference between the amplitudes of h_{SD}^{abc} found in the plaquette and in the linear cluster (Table III). The more realistic two-band model introduces an alternative mechanism, since there exist two pathways to go from $|a\bar{b}\rangle$ to $|b\bar{c}\rangle$, both involving electron-transfer processes between the Cu and oxygen atoms, (cf. Fig. 14, where sites I and II correspond to oxygen atoms).

The bottom pathway corresponds to the process appearing in the one-band model, which is not the case for the first one. Explicitly, the excitation energies are

$$\Delta E_1 = E_d - E_p - U_p = \Delta E_{CT} - U_d + \frac{2}{R}, \quad (25)$$

$$\begin{aligned} \Delta E_2 &= 2E_d - 2E_p + U_p - 2U_p - \frac{4}{R} + V_{I,II} \\ &= 2\Delta E_{CT} - U_d + V_{I,II}, \end{aligned} \quad (26)$$

$$\Delta E_3 = E_d - E_p - U_p + U_d - \frac{3}{R} + V_{a,II} = \Delta E_{CT} - \frac{1}{R} + V_{a,II}, \quad (27)$$

$$\Delta E'_1 = \Delta E_3, \quad (28)$$

$$\Delta E'_2 = U_d - \frac{2}{R} + V_{ac}. \quad (29)$$

It is likely that $\Delta E'_2 > \Delta E_2$, i.e., that the bottom pathway has a larger contribution to the singlet displacement. The overall effect is

$$h_{SD}^{abc} = \frac{t_{pd}^4}{\Delta E'_1} \left(\frac{1}{\Delta E_1} \cdot \frac{1}{\Delta E_2} + \frac{1}{\Delta E'_1} \cdot \frac{1}{\Delta E'_2} \right), \quad (30)$$

i.e., of the same order of magnitude as J_{NN} . Regarding the orientation effect it is clear that the denominators are larger

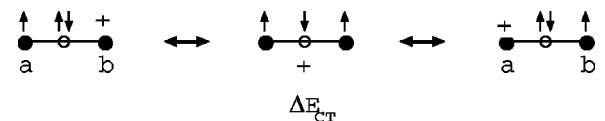


FIG. 10. Two-band model hole hopping mechanism, involving an intermediate charge-transfer state. Open circle corresponds to a bridge oxygen atom, and the closed circles to the copper atoms.

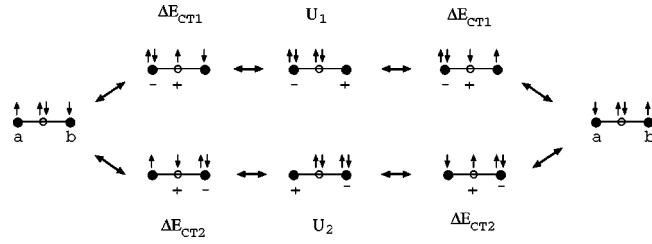


FIG. 11. Two-band model spin-exchange mechanism, with two pathways involving charge transfer states.

for the perpendicular orientation than for the linear one, due to the hole-hole repulsions $V_{I,II}$, $V_{a,II}$, and V_{ac} , and it is expected that h_{SD}^{abc} will be larger for the linear orientation, as found in the numerical *ab initio* calculations (-80 meV and -40 meV, respectively).

B. Further exploration of the influence of the hole(s) on J_{NN} and t_{NN}

In order to evaluate this influence, larger clusters would have to be considered, which is beyond our computational possibilities (the preceding CI expansions frequently reach 10^7 determinants), and a simpler procedure has to be used. In the present set of calculations, binuclear Cu_2O_7 clusters have been chosen as before, adding one or two additional point charges on Cu sites of the environment, which become Cu^{+3} centers, in order to grossly mimic the effect of the holes. For first-neighbor holes, this is a rather crude approximation, and its relevance has to be tested by comparison with the previously reported four- and three-center calculations. Actually, for a perpendicular position of the hole $J_{NN}=115$ meV (compared to 104 meV in the plaquette). For a colinear hole $J_{NN}=175$ meV, compared to 156 meV in the linear cluster. Hence the anisotropy of the first-neighbor hole is qualitatively reproduced. As an additional confirmation we have calculated the effect of two holes in the plaquette and we get the same value $J_{NN}=93$ meV as for the two-hole-containing plaquette. Table V gives the results for J_{NN} concerning a series of possibilities with one remote hole, two holes in different positions, together with the variation of the electrostatic energy in the intermediate charge transfer states with respect to the nondoped case, expressed in eV. Figure 15(a) shows the correlation between the calculated J_{NN} value with the variation of the electrostatic energy $\delta E_{CT1} + \delta E_{CT2}$ in the

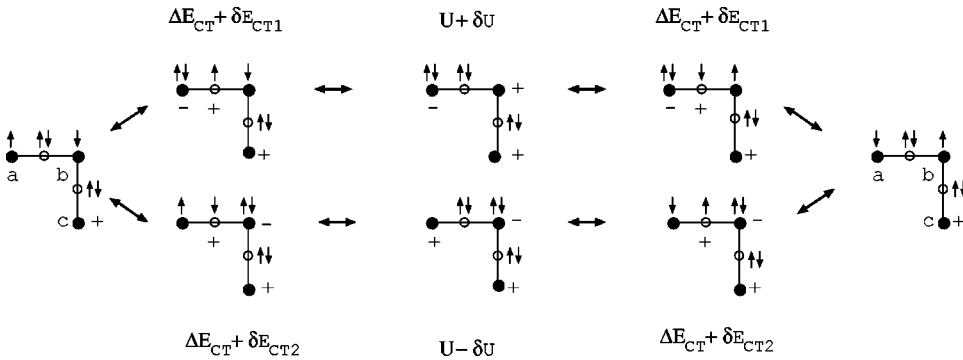


FIG. 12. Two-band model spin-exchange mechanism in presence of a hole in a perpendicular position.

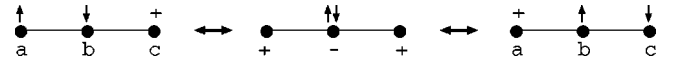


FIG. 13. One-band model representation of the singlet-displacement operator.

intermediate charge-transfer states. The correlation is quite satisfactory and suggests the following law in eV:

$$J_{NN} = 0.131 - 0.053(\delta E_{CT1} + \delta E_{CT2}). \quad (31)$$

An analogous fit of the hopping integral dependence on the variation of the electrostatic energy in the intermediate charge-transfer state $\delta E_{CT} - \delta E_0$ has been attempted from the values of t_{NN} (Table V) calculated on binuclear complexes in presence of external hole(s). The correlation is less satisfactory [Fig. 15(b)]. The distortions of the active orbitals in presence of these close holes should be non-negligible and should affect the amplitudes of the hopping integral in a rather complex manner. However, it seems simpler to search for a linear law rather than to produce and handle a dictionary of operator amplitudes considering exhaustively all possible occurrences. We therefore propose the following fit in eV for the first-neighbor hopping integral:

$$t_{NN} = -0.521 + 0.187(\delta E_{CT} - \delta E_0). \quad (32)$$

V. DISCUSSION AND CONCLUSIONS

The numerical results obtained here above suggest that the usual t - J or t - J - V model Hamiltonians neglect important physical effects, which should be incorporated into an extended model Hamiltonian. The main deviations from the t - J Hamiltonian are the following:

(i) The inclusion of the second-neighbor hopping, $t_{NNN} \approx +110$ meV. The third-neighbor interaction $t_{nNNN} \approx -40$ meV could tentatively be omitted. Recent analysis of angle-resolved photoemission spectroscopy data has shown that both t_{NNN} and t_{nNNN} are necessary for understanding the dispersion and line shape of the spectral function in the t - J model.²⁶ Tohyama *et al.*²⁵ have estimated the ratio t_{NNN}/t_{NN} and t_{nNNN}/t_{NN} to be -0.12 and 0.08 , respectively, by fitting the tight-binding Fermi surface to the experimental one in

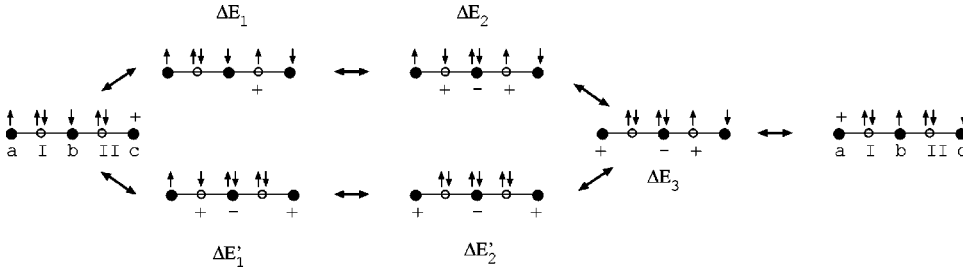


FIG. 14. Two-band model representation of the singlet-displacement operator. In this case, the mechanism involves charge-transfer intermediate states.

the overdoped sample⁵⁹ on the assumption that in the overdoped region the Fermi surface of the tight-binding band is the same as that of the t - t' - t'' - J model. The values proposed

TABLE V. Magnetic coupling and hopping integral in binuclear clusters with hole(s) in adjacent position(s) and intermediate state energies (all in eV).

	Undoped		1 Hole-doped	
	J	$\delta E_{CT1} + \delta E_{CT2}$	t	$\delta E_{CT} - \delta E_0$
	0.116	0.305	-0.450	0.152
	0.135	-0.17	-0.558	-0.084
	0.175	-0.61	-0.590	-0.305
	0.093	0.61	-0.458	0.312
	0.098	0.61	-0.482	0.305
	0.116	0.57	-0.456	0.305
	0.130	-0.14	-0.502	0.076
	0.144	-0.685	-0.593	-0.335
	0.193	-1.22	-0.691	-0.633
	0.200	-0.84	-0.563	-0.404

here are in good agreement with these ratio: $t_{NNN}/t_{NN} = -0.19$ and $t_{nNNN}/t_{NN} = 0.08$ but not with the ratio J/t_{NN} proposed by these authors ($J/t_{NN, Tohyama} = 0.4$ vs $J/t_{NN} = 0.22$).

(ii) The singlet displacement operator h_{SD} has to be taken into account, at least for the colinear displacement, since $h_{SD} \approx -80$ meV.

(iii) The hole-hole repulsion appears to be far from negligible. Due to possible screening effects and electrostatic mean cancellations by the Sr ions, it is certainly reasonable to neglect the hole-hole repulsions beyond the third neighbors. Even if the calculated values $V_{NN} - V_{NNN} = 0.8$ eV and $V_{NN} - V_{nNNN} = 1.5$ eV were somewhat exaggerated, these interactions certainly play an important role.

(iv) The magnetic coupling and hopping integral between adjacent atoms depend in a stereospecific manner on the existence and position of hole(s) in the immediate vicinity. A simple correlation with the electrostatic energies of the intermediate ligand to metal charge-transfer states has been proposed resulting in simple formulas, which should be used in

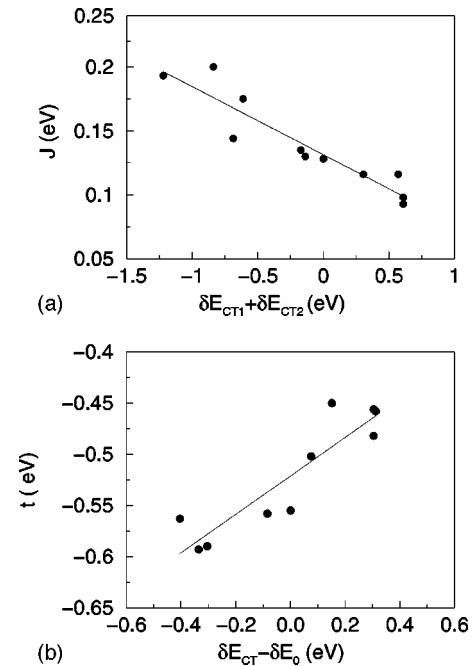


FIG. 15. Linear correlation between the calculated first-neighbor interactions in binuclear clusters and the change of the electrostatic energy in the intermediate charge-transfer states (in eV): (a) on the top, J_{NN} versus $\delta E_{CT1} + \delta E_{CT2}$; (b) on the bottom, t_{NN} versus $\delta E_{CT} - \delta E_0$.

a realistic model Hamiltonian. From the exploratory calculations appearing in Table V, and for the sake of simplicity, it seems sufficient to consider the first neighbors of the bond in the calculation of the electrostatic energy changes $\delta E_{CT1} + \delta E_{CT2}$ and $\delta E_{CT} - \delta E_0$ appearing in formulas (31) and (32), respectively.

One may therefore propose the following extended t - J model Hamiltonian:

$$\begin{aligned}
 H = & \sum_{\langle pq \rangle}^{NN} t(\delta E) \cdot (a_p^\dagger a_q + a_q^\dagger a_p + s.c.) \delta(n_p + n_q, 1) \\
 & - J(\delta E) \cdot (S_p \cdot S_q) + \sum_{\langle pr \rangle}^{NNN} t_{NNN} \cdot (a_p^\dagger a_r + a_r^\dagger a_p + s.c.) \\
 & \times \delta(n_p + n_r, 1) - J_{NNN} \cdot (S_p \cdot S_r) + \sum_{\langle pqrs \rangle}^{plaquette} K \cdot [(S_p \cdot S_q) \\
 & \times (S_r \cdot S_s) + (S_p \cdot S_s)(S_q \cdot S_r) - (S_p \cdot S_r)(S_q \cdot S_s)] \\
 & + \sum_{\langle pqr \rangle}^{connected} h_{SD}^{pqr} \cdot (a_p^\dagger a_q^\dagger a_q a_r^- + a_r^\dagger a_q^\dagger a_q a_p^- - a_p^\dagger a_q^\dagger a_r a_q^- \\
 & - a_r^\dagger a_q^\dagger a_p a_q^- + s.c.) \delta(n_p + n_q + n_r, 2) \\
 & + \sum_{pq}^{\leq nNNN} V_{pq} \cdot \delta(n_p, 0) \cdot \delta(n_q, 0).
 \end{aligned}$$

In this Hamiltonian, $t(\delta E)$ and $J(\delta E)$ reflect the dependence of the first-neighbor interactions on the number and position of the adjacent holes, which is controlled by the energy changes in the charge-transfer intermediates. The second-neighbor interactions are not influenced by the presence of adjacent holes and the displacement of a singlet takes place toward an adjacent hole, so the positions occupied by the singlet and the hole have to be connected.

The here-proposed modifications with respect to the usual t - J or t - J - V Hamiltonians are important. We would like to point out that some local physical effects evidenced in the present work may have an impact on the spatial ordering of

charges and spins and on their dynamics. In a crude static look at this problem one may notice that stripping separation of charges and spins (i) favors the mobility of holes in the charged column, since t and J values become especially larger, (ii) leads to a stronger magnetic coupling in the bonds perpendicular to the stripes (with a trend to form singlets on these bonds). The last two effects would result from the three-body corrections on t and J created by the adjacent holes. Finally, (iii) the mobility of the stripes can be enhanced by the second-neighbor hopping integral and by the singlet displacement operator.

The present work was concentrated on the La_2CuO_4 lattice only. However the here-evidenced three-body or non-nearest-neighbor two-body operators should be present in similar materials, which may present a variety of t and J values. The discussed mechanisms leading to these effects actually are not specific of the La_2CuO_4 lattice. Exploring their amplitudes on other lattices would be a valuable task. The other prospect would be to introduce our extended t - J Hamiltonian in numerical simulations of the collective properties of the lattice. It should be stressed that the bottleneck of such calculations is the length of the wave-function vector, which is unchanged with respect to the original t - J Hamiltonian, the additional terms simply slowing slightly the speed of the computations of the action of the Hamiltonian on the vector, at each iteration.

ACKNOWLEDGMENTS

The authors wish to thank Daniel Maynau for computational help and development. The ROHF calculations were done using the MOLCAS package,⁶⁰ the DDCI calculations were done using the CASDI package.⁶¹ The authors are indebted to the European Commission for the TMR network contract ERBFMRX-CT96-0079, Quantum Chemistry of Excited States. C.J.C. acknowledges financial support through the TMR activity ‘‘Marie Curie research training grants’’ Grant No. HPMF-CT-1999-00285 established by the European Commission. The Laboratoire de Physique Quantique is ‘‘Unité Mixte de Recherche UMR 5626 du CNRS.’’

*On leave from Departamento de Química Física, Universidad de Sevilla, E-41012 Sevilla, Spain.

¹P. E. Sulewski, P. A. Fleury, K. B. Lyons, S.-W. Cheong, and Z. Fisk, Phys. Rev. B **41**, 225 (1990).

²R. P. Singh, P. A. Fleury, K. B. Lyons, and P. C. Sulewski, Phys. Rev. Lett. **62**, 2736 (1989).

³G. Aeppli, S. M. Hayden, H. A. Mook, Z. Fisk, S.-W. Cheong, D. Rytz, J. P. Remeika, G. P. Espinosa, and A. S. Cooper, Phys. Rev. Lett. **62**, 2052 (1989).

⁴Y. Endoh, K. Yamada, R. J. Birgeneau, D. R. Gabbe, H. P. Jensen, M. A. Kastner, C. J. Peters, P. J. Picone, T. R. Thurston, J. M. Tranquada, G. Shirane, Y. Hidaka, M. Oda, Y. Enomoto, M. Suzuki, and T. Murakami, Phys. Rev. B **37**, 7443 (1988).

⁵S. M. Hayden, G. Aeppli, R. Osborn, A. D. Taylor, T. G. Perling, S. W. Cheong, and Z. Fisk, Phys. Rev. Lett. **67**, 3622 (1991).

⁶J. B. Parkinson, J. Phys. C **2**, 2012 (1969).

⁷C. M. Canali and S. M. Girvin, Phys. Rev. B **45**, 7127 (1992).

⁸M. Roger and J. M. Delrieu, Phys. Rev. B **39**, 2299 (1989).

⁹E. Gagliano and S. Bacci, Phys. Rev. B **42**, 8772 (1990).

¹⁰E. Dagotto and D. Poilblanc, Phys. Rev. B **42**, 7940 (1990).

¹¹F. Nori, E. Gagliano, and S. Bacci, Phys. Rev. Lett. **68**, 240 (1992).

¹²J. Eroles, C. D. Batista, S. B. Bacci, and E. R. Gagliano, Phys. Rev. B **59**, 1468 (1999).

¹³J. Lorenzana, J. Eroles, and S. Sorella, Phys. Rev. Lett. **83**, 5122 (1999).

¹⁴Y. Honda, Y. Kuramoto, and T. Watanabe, Phys. Rev. B **47**, 11329 (1993).

¹⁵T. Sakai and Y. Hasegawa, Phys. Rev. B **60**, 48 (1999).

¹⁶J. P. Malrieu and D. Maynau, J. Am. Chem. Soc. **104**, 3021 (1982).

¹⁷D. Maynau and J. P. Malrieu, J. Am. Chem. Soc. **104**, 3029 (1982).

- ¹⁸A. H. MacDonald, S. M. Girvin, and D. Yoshioka, *Phys. Rev. B* **37**, 9753 (1988).
- ¹⁹A. H. MacDonald, S. M. Girvin, and D. Yoshioka, *Phys. Rev. B* **41**, 2565 (1990).
- ²⁰V. J. Emery and G. Reiter, *Phys. Rev. B* **38**, 4547 (1988).
- ²¹F. C. Zhang and T. M. Rice, *Phys. Rev. B* **37**, 3759 (1988).
- ²²F. C. Zhang and T. M. Rice, *Phys. Rev. B* **41**, 7243 (1990).
- ²³S. White and D. J. Scalapino, cond-mat/0006071 (unpublished).
- ²⁴G. B. Martins, J. C. Xavier, C. Gazza, M. Vojta, and E. Dagotto, *Phys. Rev. B* **63**, 014414 (2001).
- ²⁵T. Tohyama, S. Nagai, Y. Shibata, and S. Maekawa, *Phys. Rev. Lett.* **82**, 4910 (1999).
- ²⁶C. Kim, P. J. White, Z.-X. Shen, T. Tohyama, Y. Shibata, S. Maekawa, B. O. Wells, Y. J. Kim, R. J. Birgeneau, and M. A. Kastner, *Phys. Rev. Lett.* **80**, 4245 (1998).
- ²⁷C. Gazza, G. B. Martins, J. Riera, and E. Dagotto, *Phys. Rev. B* **59**, R709 (1999).
- ²⁸J. Riera and E. Dagotto, *Phys. Rev. B* **57**, 8609 (1998).
- ²⁹J. H. Han, Q. H. Wang, and D. H. Lee, cond-mat/0006046 (unpublished).
- ³⁰For a recent review, see J. Orenstein and A. J. Millis, *Science* **288**, 468 (2000).
- ³¹I. de P. R. Moreira, F. Illas, C. J. Calzado, J. F. Sanz, J. P. Malrieu, N. Ben Amor, and D. Maynau, *Phys. Rev. B* **59**, R6593 (1999).
- ³²C. J. Calzado, J. F. Sanz, J. P. Malrieu, and F. Illas, *Chem. Phys. Lett.* **307**, 102 (1999).
- ³³C. J. Calzado, J. F. Sanz, and J. P. Malrieu, *J. Chem. Phys.* **112**, 5158 (2000).
- ³⁴C. Bloch, *Nucl. Phys.* **6**, 329 (1958).
- ³⁵S. F. Boys, *Rev. Mod. Phys.* **32**, 306 (1960); S. F. Boys, in *Quantum Theory of Atoms, Molecules and Solid State*, edited by P.-O. Lodwin (Academic Press, New York, 1966).
- ³⁶J. des Cloizeaux, *Nucl. Phys.* **20**, 321 (1960).
- ³⁷N. W. Winter, R. M. Pitzer, and D. K. Temple, *J. Chem. Phys.* **86**, 3549 (1987); **87**, 2945 (1987).
- ³⁸*Clusters Models for Surface and Bulk Phenomena*, edited by G. Pacchioni and P. Bagus (Plenum, New York, 1992).
- ³⁹J. Casanovas, J. Rubio, and F. Illas, *Phys. Rev. B* **53**, 945 (1996).
- ⁴⁰A. B. van Oosten, R. Broer, and W. C. Nieuwpoort, *Chem. Phys. Lett.* **257**, 207 (1996).
- ⁴¹F. Illas, I. de P. R. Moreira, C. de Graaf, O. Castell, and J. Casanovas, *Phys. Rev. B* **56**, 5069 (1997).
- ⁴²R. L. Martin and F. Illas, *Phys. Rev. Lett.* **79**, 1539 (1997).
- ⁴³H. M. Evjen, *Phys. Rev.* **39**, 675 (1932).
- ⁴⁴R. L. Martin and P. J. Hay, *J. Chem. Phys.* **98**, 8680 (1993); R. L. Martin, *ibid.* **98**, 8691 (1993); *Phys. Rev. B* **53**, 15 501 (1996); *ibid.* **54**, R9647 (1996); in *Clusters Models for Surface and Bulk Phenomena*, edited by G. Pacchioni and P. Bagus (Plenum, New York, 1992).
- ⁴⁵For instance, M. A. Nygren, L. G. M. Pettersson, Z. Barandiarán, and L. Seijo, *J. Chem. Phys.* **100**, 2010 (1994); M. Pohlchen and V. Staemmler, *J. Chem. Phys.* **97**, 2583 (1992).
- ⁴⁶For metallic atoms, the *ab initio* relativistic core model potential proposed by Barandiarán [Z. Barandiarán and L. Seijo, *Can. J. Phys.* **70**, 409 (1992)] has been used, where the Cu valence electrons are described by a $(9s6p6d)/[3s3p4d]$ basis set. For the oxygen atoms, an all electron basis set $(10s5p)$ contracted to $[3s2p]$ is employed [T. H. Dunning, Jr., *J. Chem. Phys.* **53**, 2823 (1970); T. H. Dunning, Jr. and P. J. Hay, in *Methods of Electronic Structure Theory*, edited by H. F. Schaefer III, Vol. 2 (Plenum Press, New York, 1977)].
- ⁴⁷J. Miralles, O. Castell, R. Caballol, and J. P. Malrieu, *Chem. Phys.* **172**, 33 (1993).
- ⁴⁸Two different strategies have been used to define the active orbitals, magnetic and ligand-centered orbitals. For undoped systems, where the magnetic orbitals are well represented by the Hartree-Fock eigenvectors, the ligand-centered orbitals can be rationally determined as eigenvectors of the difference of the density matrices, corresponding to the low-lying eigenstates (Ref. 49). For doped clusters, where the role of the oxygen atoms is more important, the active orbitals are redefined by means of an iterative procedure (*iterative* DDCI, IDDCI) [V. M. García, O. Castell, R. Caballol, and J. P. Malrieu, *Chem. Phys. Lett.* **238**, 222 (1995)]. Starting with the previously defined orbitals, one performs the single-excitation CI on the top of the minimal CAS. The diagonalization of the average density matrix for the relevant eigenstates provides *revised* doubly and partially occupied MO's, i.e., hole-adapted *core* orbitals and valence orbitals, with an appropriate hybridization of the Cu $3d$ and O $2p$ orbitals.
- ⁴⁹For a variational development, see C. J. Calzado, J. P. Malrieu, J. Cabrero, and R. Caballol, *J. Phys. Chem. A* **104**, 11 636 (2000). For the perturbative formulations, see J. Miralles, R. Caballol, and J. P. Malrieu, *Chem. Phys.* **153**, 25 (1991); O. Castell, R. Caballol, V. M. García, and K. Handrick, *Inorg. Chem.* **35**, 1609 (1996); C. J. Calzado, J. F. Sanz, O. Castell, and R. Caballol, *J. Phys. Chem. A* **101**, 1716 (1997).
- ⁵⁰J. Cabrero, N. Ben Amor, C. de Graaf, F. Illas, and R. Caballol, *J. Phys. Chem. A* **104**, 9983 (2000).
- ⁵¹S. Uchida, T. Ido, H. Takagi, T. Arima, Y. Tokura, and S. Tajima, *Phys. Rev. B* **43**, 7942 (1991).
- ⁵²H. Schmidt and Y. Kuramoto, *Physica C* **167**, 263 (1990).
- ⁵³M. Matsuda, K. Katsumata, R. S. Eccleston, S. Brehmer, and H.-J. Mikeska, *J. Appl. Phys.* **87**, 6271 (2000).
- ⁵⁴Y. H. Wang, M. D. Newton, and J. W. Davenport, *Phys. Rev. B* **46**, 11 935 (1992).
- ⁵⁵M. Hybertsen, E. B. Stechel, M. Schluter, and D. R. Jennison, *Phys. Rev. B* **41**, 11 068 (1990).
- ⁵⁶J. H. Van Vleck, *Phys. Rev.* **33**, 467 (1929); B. H. Brandow, *Int. J. Quantum Chem.* **15**, 207 (1979).
- ⁵⁷H. Eskes and J. H. Jefferson, *Phys. Rev. B* **48**, 9788 (1993).
- ⁵⁸R. Kirsch, A. Gérard, and M. Wautelet, *J. Phys. C* **7**, 3633 (1974).
- ⁵⁹A. Ino, C. Kim, T. Mizokawa, Z. X. Shen, A. Fujimori, M. Takaba, K. Tamasaku, H. Elisaki, and S. Uchida, *J. Phys. Soc. Jpn.* **68**, 1496 (1999).
- ⁶⁰K. Andersson, M. R. A. Blomberg, M. P. Fülcher, G. Karlström, R. Lindh, P. A. Malmqvist, P. Neogrády, J. Olsen, B. O. Roos, A. J. Sadlej, M. Schütz, L. Seijo, L. Serrano-Andrés, P. E. M. Siegbahn, and P. O. Widmark, MOLCAS version 4, Lund University, Sweden, 1997.
- ⁶¹CASDI program, N. Ben Amor, and D. Maynau, *Chem. Phys. Lett.* **286**, 211 (1998).